The Cryosphere Discuss., 7, 1871–1905, 2013
www.the-cryosphere-discuss.net/7/1871/2013/
doi:10.5194/tcd-7-1871-2013

The Cryosphere
Discussions
Open Access

Influence of regional precipitation patterns on stable isotopes in ice cores from the central Himalayas

H. Pang[1], **S. Hou**[1], **S. Kaspari**[2], **and P. A. Mayewski**[3]

[1]Key Laboratory of Coast and Island development of Ministry of Education, School of Geographic and Oceanographic Sciences, Nanjing University, Nanjing 210093, China
[2]Department of Geological Sciences, Central Washington University, Ellensburg, WA 98926, USA
[3]Climate Change Institute and Department of Earth Sciences, University of Maine, Orono ME 04469, USA

Received: 17 April 2013 – Accepted: 24 April 2013 – Published: 2 May 2013

Correspondence to: S. Hou (shugui@nju.edu.cn)

Published by Copernicus Publications on behalf of the European Geosciences Union.

Abstract

Several ice cores have been recovered from the Dasuopu Glacier and the East Rongbuk (ER) Glacier in the central Himalayas since the 1990s. Although the distance between the ER and the Dasuopu ice core drilling sites is only ~ 125 km, the stable isotopic record ($\delta^{18}O$ or δD) of the ER core is interpreted as a precipitation proxy while the Dasuopu core as a temperature proxy. Thus, the climatological significance of the stable isotopic records of these Himalayan ice cores remains a subject of debate. Based on analysis of regional precipitation patterns over the region, we find that the different interpretations of the Dasuopu and Everest isotopic records may not be contradictive. The north–south and west–east seesaws of the Indian Summer Monsoon (ISM) precipitation are primarily responsible for precipitation falling at the ER site, which results in a negative correlation between the ER $\delta^{18}O$ or δD record and precipitation amount along the southern slope of the central Himalayas, corresponding to the "amount effect". In addition to the ISM precipitation, non-summer monsoonal precipitation associated with winter westerlies also significantly contributes to precipitation falling at the Dasuopu site, which may cause a positive correlation between the Dasuopu stable isotopic record and temperature, in response to the "temperature effect". Our results have important implications for interpreting the stable isotopic ice core records recovered from different climatological regimes of the Himalayas.

1 Introduction

The Himalayas impact regional and even global climate due to their high elevation and large topography; however, climate research over the Himalayas is restricted owing to the lack or short duration of meteorological observations because of complex and challenging topographic conditions. Nevertheless, the largest volume of ice outside the polar regions in the Himalayas can preserve high-resolution and long-term climate and environment information, ascribed to low temperature and relatively high snow accumulation. To reconstruct climatic and environmental information of the past in the central Himalayas, several ice cores were recently retrieved from the East Rongbuk (ER) Glacier (27° 59′ N, 86° 55′ E; 6518 m a.s.l.), Mt. Qomolangma (Everest) (Hou et al., 2000, 2003; Kaspari et al., 2007), and the Dasuopu Glacier (28° 23′ N, 85° 43′ E; 7200 m a.s.l.), Mt. Xixiabangma (Thompson et al., 2000; Davis et al., 2005) (Fig. 1). Invaluable climatic and environmental information in the high central Himalayas has been revealed by these ice cores, such as regional warming (Thompson et al., 2000; Hou et al., 2007), atmospheric pollution induced by anthropogenic activities since the industrial revolution (Duan et al., 2007; Kaspari et al., 2009b; Hong et al., 2009), precipitation variations over the central Himalayas (Duan et al., 2004; Kaspari et al., 2008), atmospheric dust deposition over the past several centuries (Kaspari et al., 2009a; Xu et al., 2010), black carbon concentrations (Ming et al., 2008; Kaspari et al., 2011) and bacterial information (Zhang et al., 2007, 2008).

Ice core stable isotopes (δ^{18}O and δD, the water stable isotopic compositions expressed in δ units per mille versus VSMOW, the Vienna Standard Mean Ocean Water) are a fundamental and important proxy for temperature (i.e., temperature effect, a positive correlation between stable isotopic composition in precipitation and temperature) or precipitation (i.e., amount effect, a negative correlation between stable isotopic composition in precipitation and precipitation amount) (Dansgaard, 1964). Although stable isotopes in ice cores from the central Himalayas have been investigated for more than a decade, there is a discrepancy in the interpretation of the Himalayan ice core isotopic record. According to previous studies, the ER ice-core stable isotopic record is generally interpreted as a proxy for precipitation amount related to the Indian Summer Monsoon (ISM) (Zhang et al., 2005; Kaspari et al., 2007), whereas the Dasuopu core is interpreted as a proxy for temperature (Thompson et al., 2000; Davis et al., 2005). The East Rongbuk and Dasuopu glaciers are both located in the central Himalayas (the distance between them only 125 km) and the large-scale atmospheric circulation (the ISM and winter westerlies) at the two sites are the same. Furthermore, seasonal variations of ice-core δ^{18}O (or δD) at the two sites are similar: high δ values in winter and low values in summer (Wang et al., 2008; Pang et al., 2012). Why do the different interpretations of the stable isotopic records from the two cores occur? Are there any climatological differences between the two sites to justify the different interpretations that have been presented?

In this paper, we clarify the influence of regional precipitation patterns on the central Himalayan ice core stable isotopic records. Precipitation patterns over the region are investigated utilizing meteorological observations along the Himalayas, monthly NCEP/NCAR (National Centers for Environmental Prediction/National Center for Atmospheric Research) reanalysis data, instrumental summer monsoon rainfall series of the Indian regions, and the ER and Dasuopu δ^{18}O and accumulation rate records. The paper consists of: Sect. 2, the atmospheric circulation systems over the Himalayas; Sect. 3, the data used; Sect. 4, regional precipitation patterns and their impacts on the ice core stable isotopic record: Sect. 5, the possible mechanisms for regional precipitation patterns; Sect. 6, the discussion; and Sect. 7 the conclusions.

2 Atmospheric circulation systems in the study area

The Himalayas, the world's highest mountains, are located at the southern edge of the Tibetan Plateau (TP), with a total length of ~2500 km from Mt. Nanga Parbat in the west to Mt. Namjagbarwa in the east. The Himalayas intercept considerable moisture due to the topographic blocking effect. During the summer monsoon season (June to September), the ISM transports large amounts of water vapor from the Indian Ocean to the Himalayas and the southern TP via two monsoon moisture trajectories: one from the Indian Ocean across the Arabian Sea, and along the Indian River valley to the western Himalayas and TP; the other from the Bay of Bengal moving northward to the eastern Himalayas and TP along the Brahmaputra River valley (Liu, 1989; Lin and Wu, 1990) (Fig. 1). During the non-summer monsoon season (October to May), winter westerlies bifurcate into the northern and southern branches around the TP (Fig. 1), the latter affecting the Himalayas and southern TP (Wei and Gasse, 1999). Wintertime precipitation in the Himalayas is related to vapor transport by the southern branch. The weather systems responsible for wintertime precipitation in the Himalayas are the Western Disturbances, westerly upper-tropospheric synoptic-scale waves (Gupta et al., 1999), and low-pressure systems that set up a favorable large-scale environment (e.g., lower temperature, higher humidity and upward vertical motion) for winter snowfall in the Himalayas (Lang and Barros, 2004).

3 Data

The annually-dated ER ice core was drilled in 2002 with a depth of 108.8 m. The core was maintained at $< -5^{\circ}$ from the time of drilling until analysis. Measurements of δ^{18}O of the core were performed by a Finnigan delta-plus mass spectrometer (precision 0.05‰) at the State Key Laboratory of Cryospheric Science, Chinese Academy of Sciences. The ice core was annually dated to the year 1534 AD at the depth of 98 m. Correspondingly, the annually snow accumulation rate since 1534 AD was recovered by Kaspari and co-authors (Kaspari et al., 2008). Details about this core, including sampling processing, laboratory analysis and dating, can be found elsewhere (Kaspari et al., 2007, 2008). In 1997, three ice cores were recovered from the Dasuopu glacier. The third one (Core 3), 167.7 m long, was drilled to bedrock at the summit of the glacier (Thompson et al., 2000). The $\sim$560 yr records of annually averaged δ^{18}O (1450–1996 AD) and accumulation rate (1442–1996 AD) are available from the NOAA National Climatic Data Center for Paleoclimatology (http://www.ncdc.noaa.gov/paleo/paleo.html). The instrumental summer monsoon rainfall series of Indian regions during 1813–2006 AD (i.e., NEI: North East India; NCI: North Central India; NWI: North West India; NMI: North Mountainous India; WPI: West Peninsular India; EPI: East Peninsular India; SPI: South Peninsular India; AISMR: All Indian Summer Monsoon Rainfall) (Fig. 1) are available from the Indian Institute of Tropical Meteorology at www.tropmet.res.in (Sontakke and Singh, 1996; Sontakke et al., 2008). In order to compare with the Indian instrumental summer monsoon rainfall series, the ER and Dasuopu ice core $\delta^{18}O$ and accumulation rate since 1813 AD are used in this paper. Additionally, the monthly precipitation amount data from four Himalayan meteorological stations (Pali, Dingri, Nyalam and Pulan Stations, Fig. 1) used here are available from the China Meteorological Data Sharing Service System. Lastly, the monthly NCEP/NCAR reanalysis data (outgoing long-wave radiation (OLR), air temperature at multiple levels and sensible heat net flux) with $2.5^{\circ} \times 2.5^{\circ}$ resolution were obtained from the NOAA/ESRL PSD (National Oceanic and Atmospheric Administration/Earth System Research Laboratory, Physical Sciences Division) at www.esrl.noaa.gov/psd/data/reanalysis (Kistler et al., 2001).

4 Regional precipitation patterns and their impacts on the Himalayan ice core stable isotopic record

4.1 Seasonal distribution of precipitation along the Himalayas

In order to reveal the nature of the different climatological interpretations of the stable isotopic records from ER and Dasuopu cores, time series of ice-core $\delta^{18}O$ and accumulation rate from the two sites are compared (Fig. 2). The trend in the ER accumulation rate is opposite to that of Dasuopu and the average accumulation rate at Dasuopu (1.28 m i.e.) is almost three times the rate at ER (0.44 m i.e.). In addition, the ER and Dasuopu accumulation rates show step changes: higher values (the average 1.55 m i.e.) before 1900 AD and lower values (the average 1.04 m i.e.) with significant decrease trend after 1900 AD at the Dasuopu site; while lower values (the average 0.32 m i.e.) before 1900 AD and higher values (the average 0.53 m i.e.) with a significant increase trend after 1900 AD at the ER site (Fig. 2). On the other hand, the increasing linear trend of Dasuopu $\delta^{18}O$ is significant (at 99 % confidence level), which was interpreted as an indicator of rising temperature by some researchers (Thompson et al., 2000; Yao et al., 2006). However, such an increasing trend is not significant for the ER $\delta^{18}O$ record. Furthermore, the ER $\delta^{18}O$ even shows decrease a trend to more

TCD
7, 1871–1905, 2013

negative δ^{18}O since the 1930s to the late 1980s (Fig. 2). The remarkable difference in the snow accumulation rate reconstructed from the ER and Dasuopu cores suggests that the major precipitation origins of the two sites may differ, which could account for the differences in ER and Dasuopu isotopic records.

To discern the precipitation difference between the ER and Dasuopu sites, the seasonal distribution of precipitation at the four weather stations, Pali (27°44′ N, 89°05′ E, 4300 m a.s.l.), Dingri (28°38′ N, 87°05′ E, 4300 m a.s.l.), Nyalam (28°11′ N, 85°58′ E, 3810 m a.s.l.) and Pulan (30°17′ N, 81°15′ E, 4900 m a.s.l.) along the Himalayas (Fig. 1), is presented in Fig. 3. The precipitation distribution over the eastern (western) Himalayas is unimodal (bimodal). Most precipitation over the eastern Himalayas occurs during the ISM season (June to September), whereas precipitation over the western Himalayas takes place during the winter/spring and summer seasons.

The difference in the seasonal distribution of precipitation between the western and eastern Himalayas must have an important impact on the Himalayan ice core stable isotopic records, because the stable isotopic composition in summer monsoonal precipitation is controlled by the "amount effect", whereas the stable isotopic ratio in non-summer monsoon precipitation is dominated by the "temperature effect" (Tian et al., 2003, 2007). The wintertime precipitation associated with winter westerlies at Nyalam station accounts for 52 % of total annual precipitation. This site is nearby Dasuopu glacier, thus we speculate that the proportion of wintertime precipitation at the Dasuopu core is also considerable. As a result, the stable isotopic record in the Dasuopu core is influenced substantially by winter westerlies. On the other hand, the proportion of summertime precipitation at Dingri station accounts for more than 90 % of the annual precipitation. Dingri is nearby the ER glacier, thus we suggest that summer monsoonal precipitation dominates accumulation at the ER glacier, and the ER stable isotopic record is mainly controlled by the ISM. Thus, the different seasonal distribution of precipitation between the western and eastern Himalayas is likely the main reason for the different climatological interpretations of the ER and Dasuopu ice-core stable isotopic records.

4.2 Spatial patterns of the ISM precipitation

It is well-known that the ISM is subject to many external and internal forces, such as solar radiation (Kodera, 2004; Neff et al., 2001; Fleitmann et al., 2003), Eurasian snow cover (Barnett et al., 1988; Verneakar et al., 1995), the El Niño/Southern Oscillation (ENSO) (Webster et al., 1998), the Indian Ocean Dipole (IOD) (Saji et al., 1999) and the Tibetan Plateau land thermal effect (Zhao et al., 2001; Wu et al., 2012). As a result, ISM precipitation exhibits large spatial variability on intraseaonal and interannual scales (Krishnamurthy and Shukla, 2000; Gadgil, 2003). To investigate spatial patterns of the ISM precipitation and associated impacts on the ER and Dasuopu ice core stable isotopic records, Empirical Orthogonal Function (EOF) and correlation analyses were conducted using the instrumental area-averaged summer monsoon (June to September) rainfall data, including all-India summer monsoon rainfall (AISMR) and summer rainfall series of Indian seven zones (i.e., NEI, NCI, NWI, NMI, WPI, EPI, and SPI), and the ER and Dasuopu δ^{18}O and accumulation rate records. The result of EOF and correlation coefficients are presented in Tables 1 and 2, respectively.

EOF1, accounting for 24.4 % of the total variance, is mainly loaded with AISMR, NCI, NWI and NMI. It represents the summer monsoon precipitation over the core Indian monsoon region, reflecting the activity of the Indian monsoon heat low (Gadgil, 2003). EOF2 accounts for 14.7 % of the total variance, loaded with WPI and EPI, representing precipitation over the middle Indian peninsula. Dasuopu δ^{18}O dominates EOF3, explaining 9.0 % of the total variance, resulting from precipitation events that can occur year round. EOF4 is loaded with SPI, explaining 9.0 % of the total variance, which represents the summer precipitation over the southern India peninsula. The relatively weak correlations between the SPI precipitation and precipitation over other Indian regions (Table 2) suggest that the SPI precipitation differs from other Indian regions. EOF5 (8.9 % of the total variance) is loaded with NEI, indicating the summer precipitation over northeast India. The poor correlations between the NEI precipitation and that over other Indian regions (Table 2) indicate that the NEI precipitation is distinct from

TCD
7, 1871–1905, 2013

other Indian regions. EOF6 (8.5 % of the total variance) is indicated by Dasuopu accumulation rate, representing the local precipitation at Dasuopu glacier. EOF7 (8.5 % of the total variance) is loaded with the ER accumulation rate, indicating the local precipitation at the ER glacier. EOF8 (8.4 % of the total variance) is loaded with the ER δ^{18}O, resulting from precipitation events that can occur year round, but are largest during the summer monsoon season. EOF analysis indicates that the δ^{18}O and accumulation rate records at the ER site are independent of those at the Dasuopu site, which support the differences of the δ^{18}O and accumulation rate records at the two sites as indicated in Fig. 2. Furthermore, the high altitudinal Himalayan ice core δ^{18}O and accumulation rate records are independent of the low altitudinal Indian summer monsoon rainfall series, which may indicate spatial heterogeneity of the ISM precipitation.

In order to further decipher the relationship between the ISM rainfall and the Himalayan ice-core isotopic and accumulation rate records, correlation coefficients between the Indian summer monsoonal rainfall series and the Himalayan ice-core δ^{18}O and accumulation rate records are included in Table 2. Positive correlations occur between the ER accumulation rate and summer monsoon rainfall over NWI, WPI, EPI, SPI and AISMR, but the correlations are not significant between the ER δ^{18}O record and summer monsoon rainfall over the Indian regions (excepting for the SPI). However, the ER δ^{18}O is negatively correlated with summer precipitation amount along the central Himalayas (Fig. 4), again confirming the “amount effect” of precipitation isotopes at the ER glacier. As for the Dasuopu core, there are no significant positive correlations between the Dasuopu accumulation rate and summer monsoon rainfall over the Indian regions, while weak negative correlations can be observed between the Dasuopu accumulation rate and rainfall over WPI, SPI and AISMR (Table 2). At the same time, there are also no significant correlations between the Dasuopu δ^{18}O record and summer monsoon rainfall over the Indian regions (excepting for the NCI). The above correlation analysis results suggest that the relationship between the Indian summer monsoonal rainfall and the ER core δ^{18}O and accumulation rate exists, but the relationship is vague for the Dasuopu core. This supports our interpretation that the ER site is mainly controlled by the ISM, while the Dasuopu core is both influenced by the ISM and winter westerlies.

The EOF and correlation analyses imply that the ISM precipitation can be generally divided into three distinct regions: the ISM core region (represented by the NWI), the northeastern region of the ISM (represented by the NEI) and the southern region of the ISM (represented by the SPI). Based on summer monsoon rainfall of rain gauges from Indian districts, Singh et al. (1992) found that the rainfall in northwest India shows a significant increasing trend and that for northeast India a significant decreasing trend over the period 1871–1984 AD. From Table 2, we can see that the summer precipitation over NEI is negatively significantly correlated with NWI precipitation. The reverse variation of precipitation between northwest and northeast India is likely indicative of an west–east oscillation of the ISM precipitation. In addition, Naidu et al. (2009) indicated that meteorological subdivisions of India are demarcated by 20° N latitude, with the regions south of it showing an increasing trend of monsoon rainfall, while most of the subdivisions to its north showing decreasing trends in the today's warming period (1970–2005 AD). For a longer timescale, Kaspari et al. (2007) revealed the weakening of the ISM in the northern high elevation region since ∼ 1400 AD, while the strengthening of the ISM in the southern low elevation were found by other researchers (Anderson et al., 2002; von Rod et al., 1999). These investigations suggest that the ISM activity probably shows a north–south seesaw.

Outgoing longwave radiation (OLR) is closely related to precipitation factors, such as cloud cover, convection intensity, vertical motion and latent heat. In general, low OLR values correspond to strong convective activity (resulting in high precipitation), while high OLR values are associated with weak convective activity (resulting in low precipitation) (Prasad and Bansod, 2000). In order to further substantiate the spatial patterns of the ISM precipitation, the composite analyses of precipitation over the SPI and NWI were performed using the large-scale NCEP/NCAR OLR reanalysis data. We define years with higher and lower precipitation over the SPI and NWI during 1974–2006 AD for composite analysis because the OLR data are available since June 1974. The sum-

TCD
7, 1871–1905, 2013

mer precipitation was standardized by subtracting the mean and dividing by the standard deviation (SD). A year with a value > 1.0 SD is defined as a year with higher precipitation, while a value < −1.0 SD is defined as a year with lower precipitation. Based on this division, there are 6 yr with higher SPI precipitation (1975, 1981, 1983, 1988, 1991 and 1996) and 5 yr with lower SPI precipitation (1976, 1987, 1990, 1999 and 2002); and there are 8 yr with higher NWI precipitation (1975, 1976, 1977, 1978, 1983, 1988, 1990 and 1994) and 5 yr with lower NWI precipitation (1974, 1979, 1987, 1991 and 2002). Figure 5 shows the difference in summer mean of OLR (June to September) between years with higher and lower summer precipitation over the SPI (Fig. 5a) and NWI (Fig. 5b).

Negative OLR anomalies occur in the southern ISM region, namely the tropical Indian Ocean; whereas positive OLR anomalies occur in the northern ISM region, especially in the northeastern India (Fig. 5a). The spatial pattern suggests that in years with higher SPI precipitation, convection activity is stronger over the southern ISM region and weaker over the northern ISM region, and in years with lower SPI precipitation, convection activity is weaker (stronger) over the southern (northern) ISM region. Previous investigations pointed out that there are two favorable locations for convection activity during the ISM season, one centralizing over the continent and the other over the equatorial Indian Ocean (Walister and Gautier, 1993; Chandrasekar and Kitoh, 1998). The observed north–south oscillation of the ISM precipitation, also reported by other researchers (Krishnamurthy and Shuka, 2000; Li and Zeng, 2002), is indicative of the north–south fluctuation of the two convection activities.

Negative OLR anomalies occur in the western ISM region, with two anomaly centers over the northwest India and the western tropical Indian Ocean, whereas positive anomalies take place in the eastern ISM region, with two anomaly centers over the northeastern India and the eastern tropical Indian Ocean (Fig. 5b). The spatial pattern indicates that in years with higher NWI precipitation, convection activity over the western ISM region is stronger and weaker over the eastern ISM region, and vice versa.

TCD
7, 1871–1905, 2013

The result is consistent with the observed west–east fluctuation of the ISM precipitation (Singh et al., 1992; Saji et al., 1999; Raju et al., 2002).

The ISM north–south and west–east seesaws suggest that when the monsoon is strong in one region it weakens in another. Monsoon rainfalls at both ends of the seesaw balance each other. Furthermore, monsoon rainfall in seesaw middle is both influenced by rainfalls at both ends of the seesaw. As a result, the Indian monsoon rainfall exhibits pronounce spatial variations and trends (Subbaramayya and Naidu, 1992). The weak positive correlations between the ER accumulation rate and precipitation over some Indian regions (Table 2) are probably resulted from the ISM spatial variations. Although the Indian summer precipitation is influenced by the north–south seesaw, the negative correlation between the ER δ^{18}O and precipitation over the northern India is still significant (Fig. 4) because the ER core is located in the northern end of the seesaw. In the west–east direction, the correlations between the ER δ^{18}O and precipitation over NWI (west end of the ISM west–east seesaw) and NEI (east end of the seesaw) are not significant (Table 2 and Fig. 4). However, the correlations are significant over the middle-northern India (Fig. 4), which may reflect the influence of the ISM west–east seesaw.

5 Potential mechanisms for regional precipitation patterns

5.1 Difference in seasonal distribution of precipitation along the Himalayas

During the winter season, precipitation over the Himalayas primarily originates from western disturbances that originate as cut-off lows (i.e., a closed low which has become completely displaced (cut off) from and moves eastward independently of the basic westerly current) over the region adjoining the Caspian Sea (Rao, 2003). These systems intrude into the western Himalayas via the notch (30–32.5° N, 70–75° E) formed by the Himalayas and Hindu Kush mountains (Lang and Barros, 2004). Many disturbances are split into two or more secondary systems by interaction with the mountains in the western Himalayas when they migrate eastward. Snowstorms are generally related to the terrain-locked low-pressure disturbances. As a result, most moisture may precipitate over the western Himalayas because of the orographic capture of snowstorms, leading to more wintertime precipitation over the western Himalayas than over the eastern Himalayas, as shown in Fig. 2.

A numerical simulation of a representative snow event suggests that significant wintertime precipitation over the central Himalayas only occurs when the western disturbances evolve to a favorable geometry with respect to the mountains (Lang and Barros, 2004). The Dasuopu core was drilled on the col of Mt. Xixiabangma, located on a ridge that extends in a northwest–southeast direction. The ridge orientation provides a favorable terrain for interacting with the western disturbances, which could cause significant wintertime precipitation at the Dasuopu core site. On the other hand, the ER core was drilled on the northeast saddle of Mt. Qomolangma (Everest), which is located on the northern slope of the Himalayan ridge. It provides an unfavorable topography for interacting with the disturbances, and thus with less wintertime precipitation at the ER core site. Therefore, the Dasuopu core site may be more heavily influenced by western disturbances than the ER core site. The mean accumulation at the Dasuopu core is much greater than at the ER core (Fig. 2), which supports our conjecture.

5.2 North–south and west–east seesaws of the ISM precipitation

5.2.1 North–south seesaw

On the intraseasonal time scale, the monsoon is considered a manifestation of the seasonal migration of the intertropical convergence zone (ITCZ, corresponding to convective cloudbands) (Gadgil, 2003). When the ITCZ is located in the equatorial Indian Ocean, it is called an equatorial trough, while it is called an Indian monsoon trough when it propagates northward onto the Indian subcontinent. The northward propagation of the ITCZ from the equatorial Indian Ocean to the Indian monsoon region occurs over 2–6 weeks (Yasunari, 1981; Gadgil and Asha, 1992). Because the cloudbands over the equatorial Indian Ocean occurs over the same longtitudinal belt as the continental cloudbands, there is a thermodynamic competition between them, leading to active spells of one being associated with weak spells of the other (Waliser and Gautier, 1993; Chandrasekar and Kitoh, 1998). Consequently, the distribution of the occurrence of ITCZ cloudbands over the ISM region is bi-modal, which may be the main reason for the observed north–south seesaw of the ISM precipitation. Nevertheless, the timescale of the observed north–south fluctuations of the ISM discussed in this paper is interannual. Can the mechanism of the intraseasonal north–south ISM oscillations still work at the interannual timescale? Although the nature of the relationship between interannual and intraseasonal variations of the ISM precipitation has remained elusive so far, some studies demonstrated that the intraseaonal oscillations play a major role in determining the annual variation of the ISM precipitation by modulating the strength and duration of active/break spells of the ISM (Goswami et al., 2003; Goswami, 2005). Furthermore, it was reported that the spatial patterns of the intraseasonal and interannual variation of ISM are highly correlated (Palmer, 1994; Ferranti et al., 1997). As a result, it is reasonable to consider that the intraseasonal oscillations in the ITCZ contribute significantly to the observed north–south seesaw of annual ISM precipitation.

Concerning the northward migration of the equatorial ITCZ into the Indian monsoon region, different mechanisms for the ITCZ northward migration have been put forward, such as the cloudiness gradient mechanism (Sikka and Gadgil, 1980), the impact of SST anomalies south of the equator over the Indian Ocean (Chandrasekar and Kitoh, 1998), changes in radiative heating in the stratosphere (Kodera, 2004) and the cycle cold air intrusion from the polar region toward the equatorial zone (Yasunari, 1981). Evidently, the south center of convective activity over the equatorial Indian Ocean and the north center over south Asia are both thermodynamically forced. Thus, the competition between them is likely based on the thermodynamic equilibrium of the whole low-pressure system from the tropical Indian Ocean to the subtropical south Asia. To test our conjecture, the summer mean mid-upper troposphere (500–200 hPa) temperatures over the tropical Indian Ocean (50–100° E; 10° S–10° N) and over the subtropical south

Asia (50–100° E; 25–40° N) are calculated based on the NCEP/NCAR air temperature data, as shown in Fig. 6a and b. It is of interest that the mid-upper troposphere temperature over the tropical Indian Ocean is positively correlated ($r = 0.251$, $p = 0.045$) with that over the subtropical south Asia, indicating consistency of thermal processes between them. However, the completely reverse linear trend between them (Fig. 5a and b) validates the thermal competition between the south convective activity over the equatorial Indian Ocean and the north one over the subtropical south Asia, supporting the observed north–south seesaw of the ISM precipitation.

5.2.2 West–east seesaw

The north–south seesaw of the ISM precipitation suggests that the ISM could be divided into two parts: the southern part of the ISM (about south of 20° N) associated with the equatorial trough and the northern part (about north of 20° N) related to the Indian monsoon trough. In the northern ISM region, there are two high and huge terrains: the Tibetan Plateau (TP) in the east and the Iranian Plateau (IP) in the west. The TP has long been considered to serve as an elevated heat source that drives the thermally direct circulation of the ISM (Ye, 1982; Zhao and Chen, 2001; Duan and Wu, 2005). Nevertheless, less consideration of the thermal effect of the IP has been addressed. More recently, it has been demonstrated that the ISM is controlled mainly by thermal forcing (surface sensible heating): the eastern part of the northern ISM region by the thermal forcing of the TP and the western part of the northern ISM by the thermal forcing of the IP (Wu et al., 2012). In order to detect whether surface sensible heating of the TP and IP can influence the west–east oscillation pattern of the northern part of the ISM, sensible heat net flux on the TP (80–102.5° E; 27.5–40° N) and on the IP (50–70° E; 27.5–37.5° N) over the period 1948–2011 was computed using the NCEP/NCAR reanalysis data, as shown in Fig. 6c and d. It is clear that sensible heat net flux on the TP is significantly reverse ($r = -0.358$, significance at 99 % confidence level, 5 yr running means) to that on the IP. Besides, the bimodality (the TP mode and the IP mode) of the 100 hPa South Asia High (SAH) found by Zhang et al. (2002) has the feature of warm preference (the SAH center is corresponding to the anomalous ascending motions and the anomalous warm column), which further proves the difference in surface sensible heating between the TP in the east and the IP in the west and its role in the northern part of the ISM. As a result, the difference of surface sensible heating between the TP and the IP is probably one key factor for the observed west–east seesaw of the northern ISM precipitation.

Nevertheless, oceanic processes (e.g., SST anomaly) are also an important factor that could influence the ISM. By analyzing sea surface temperature anomalies (SSTA) in the tropical Indian Ocean, a dipole oscillation (Indian Ocean Dipole, IOD) was first found by Saji et al. (1999). They defined an index of the IOD as the difference in SSTA between the western tropical Indian Ocean (50–70° E, 10° S–10° N) and the eastern tropical Indian Ocean (90–110° E, 10° S–equator). The IOD has two patterns: a positive phase (higher SST in the western tropical Indian Ocean) and a negative phase (higher SST in the eastern tropical Indian Ocean). A positive IOD phase leads to drought over the Indonesian region, and to heavy rain and flooding in east Africa, whereas a negative IOD causes rain and flooding in Indonesia and drought in East Africa, suggesting the significant influence of the IOD on the west–east distribution of precipitation over the southern part of the ISM. Could the west–east seesaw of precipitation over the north part of the ISM be influenced by the IOD? To answer this question, the correlation between the IOD index (calculated by the NOAA extended reconstructed SST dataset since 1854, Kaplan et al., 1998) and the summer NEI precipitation over the period 1854–2006 was calculated. The significant negative correlation between them ($r = -0.268$, $p < 0.01$) substantiates the influence of IOD on the west–east oscillation of precipitation over the northern region of the ISM. Additionally, Raju et al. (2002) suggested that the Arabian Sea branch of the ISM (the Arabian monsoon) is more vigorous (stronger cross equatorial flow) during the positive IOD phase, whereas the eastern Bay of Bengal branch of the ISM (the Bengal monsoon) is stronger (weaker cross equatorial flow) during a negative IOD phase. The fact that the Arabian monsoon waxes while the Bengal monsoon wanes, and vice versa, indicates a manifestation of

TCD
7, 1871–1905, 2013

the west–east seesaw of the northern part of the ISM. Consequently, the IOD could be another important factor for the observed west–east seesaw of the northern ISM precipitation.

6 Discussion

The different interpretations of the stable isotopic records of the ER and Dasuopu ice cores may be attributed to the contrasting seasonal distributions of precipitation at the two sites. Much larger accumulation rate at the Dasuopu core than at the ER core is probably an indicator of the different precipitation seasonality. The negative correlation between the ER and Dasuopu accumulation rates (Table 2) and their opposite linear trends (Fig. 2) are probably indicative of interplay between the westerlies and the ISM as indicated by An et al. (2012) and Yao et al. (2012). They demonstrated that there exists a reverse relationship between the westerlies and Asian summer monsoon. The high (low) Dasuopu accumulation rate before (after) 1900 AD suggests the westerlies may strengthen in a cold climate state (part of the little ice age) and weaken in a warm climate state (the anthropogenic global warming). On the contrary, the low (high) ER accumulation rate before (after) 1900 AD indicates that the ISM may weaken in a cold climate and intensify in a warm climate.

Local favorable topographic condition for interacting with the western disturbances at Dasuopu glacier leads to more wintertime precipitation there, which may be a key factor accounting for the difference in the snow accumulation rate at the two sites. In addition, there is a difference in elevation (about 700 m) between the two sites. In the high Himalayas, moisture advection associated with winter westerlies or ISM may differ with different heights. For instance at Mount Logan, low elevations receive moisture from precipitation from a high latitude source region, while higher elevations receive moisture from precipitation from a low latitude source region (Holdsworth et al., 1991; Moore et al., 2003). Correspondingly, stable isotopes (δ^{18}O and δD) versus altitude profiles indicate staircase structure, separating a lower region of altitude isotopic fractionation

TCD
7, 1871–1905, 2013

between 1750 and 3350 m from another apparent fractionation sequence appearing above 5300 m (Holdsworth et al., 1991). Some studies indicate that most annual precipitation at low altitudes of the central Himalayas falls during the ISM season (Shrestha 2000; Lang and Barros, 2004), while at high altitudes in the central Himalayas Lang and Barros (2004) found that high elevations (> 3000 m a.s.l.) can receive up to 40 % of their annual precipitation during winter. The result seems to imply that wintertime precipitation associated with the western disturbances in the central Himalayas increases with increasing elevation. For summer monsoon precipitation related to the ISM in the high elevations of Himalayas, the monsoonal precipitation amount may be restricted by the convection height of ISM. Convection frequency at lower elevations may be larger than at higher altitudes. As a result, more wintertime precipitation and less summer monsoon precipitation at the Dasuopu site are possible because its elevation is higher than at the ER site. Thus, altitudinal differences in monsoon versus westerly moisture may be another factor contributing to the seasonal difference in precipitation distribution at the two sites. However, more observations on moisture transport and precipitation at different elevations in the Himalayas are needed to verify what we assume.

Local interaction between the western disturbances and topography and potential altitudinal differences in monsoon versus westerly moisture transport both suggest that moisture sources of the ER and Dasuopu sites differ seasonally: the higher accumulation at Dasuopu may be caused by larger contributions of winter snow deposition from winter westerlies, while the prominently lower accumulation at the ER site may be dominated by the ISM. This is further supported by the ER and Dasuopu deuterium excess (d-excess = $\delta D - 8\delta^{18}O$) records. The d-excess values in ISM precipitation are generally low due to limited kinetic evaporation over the Indian Ocean under high surface air humidity, while the d-excess values in precipitation associated with winter westerlies are rather high owing to continental moisture recycling in dry climatic condition (Froehlich et al., 2008). Previous investigations suggest that the d-excess values of snow pit samples from Dasuopu glacier as high as 17.3‰, and 17.5‰ in precipitation samples (Tian et al., 2001). Additionally, the 1000 yr d-excess from Dasuopu ice core record varies between 10 and 17‰ (Tian et al., 2005). The averaged d-excess value of the ER core over the period 1813–2001 AD, 9.3‰, is much lower than that of the Dasuopu core, implying the more important contribution of precipitation from winter westerlies at Dasuopu. Tian et al. (2005) also argued that the large portion of precipitation at Dasuopu glacier is from westerly transport. Therefore, larger contributions of winter snow deposition from the westerlies could be the main reason why the Dasuopu stable isotopic record is interpreted as temperature. Thus, the past different interpretations for the stable isotopic records at the ER and Dasuopu cores may be not contradictive.

The results in Sect. 4.2 suggest that intraseasonal variability of the ISM may play an important role in the ER core stable isotopic record, which has attracted less attention before. Over seasonal time-scales or longer, the intraseaonal oscillations of the ISM are often thought to be smoothed or hidden, which is why most paleoclimate investigators usually neglect the intraseasonal fluctuations when they interpret the stable isotopic records of ice cores or speleothems from the monsoon region. However, spatial patterns of the ISM precipitation are mostly associated with intraseasonal fluctuations of the monsoon circulation. According to our analysis, we know clearly that the ISM can be divided into two parts in the north–south direction: the northern part (the Indian monsoon related to the Indian monsoon trough) and the southern part (the tropical monsoon associated with the equatorial Indian Ocean trough). Further, the northern part of the ISM consists of two branches in the west–east direction: the Arabian Sea monsoon mainly due to the thermal forcing of the IP and the Bengal monsoon mainly due to the thermal forcing of the TP. Evidently, spatial patterns of the monsoon circulation and their mechanisms should be considered when interpreting the stable isotopic records of ice cores and speleothems in Asian summer monsoon regions.

7 Conclusions

At the ER ice core site, most precipitation occurs during the ISM season, which leads to the dominance of "amount effect" on the stable isotopic record of the ER ice core. However, for the Dasuopu ice core, non-monsoon precipitation associated with winter westerlies is more important, which causes the dominance of the "temperature effect" on the Dasuopu stable isotopic record. Therefore, the past different interpretations of the stable isotopic records for the two sites may not be incompatible.

There exists two centers of convective activity in the ISM region: one over the equatorial Indian Ocean in the south and the other over the Indian sub-continent in the north. They compete for moisture and heat during the summer monsoon season, leading to the north–south oscillation of ISM precipitation. The west–east difference in thermal forcing over the ISM region, namely the different surface heating on the TP in the east and on the IP in the west, as well as the SST anomaly between the western and eastern tropical Indian Ocean, causes the west–east fluctuation of the northern ISM precipitation. The north–south and west–east seesaws of the ISM precipitation make it clear that why the ER core stable isotopic record correlates with precipitation amount over the middle-northern India, and with no significant correlations with precipitation over all Indian summer monsoon region and its sub-regions. Therefore, the spatial patterns of the ISM precipitation should be taken into account when interpreting the Himalayan ice core stable isotopic records.

Acknowledgements. This work was jointly supported in China, by National Basic Research program of China (2010CB951401), the Chinese Academy of Sciences (XDB03030101-4), National Natural Science Foundation of China (41171052 and 41176165), Fundamental Research Funds for the Central Universities (1082020904). In United States, by the US National Science Foundation (ATM 0139491 and ATM0754644). We are grateful to many scientists, technicians, students and porters for their hard work in the field.

References

An, Z., Colman, S. M., Zhou, W., Li, X., Brown, E. T., Timothy Jull, A. J., Cai, Y., Huang, Y., Lu, X., Chang, H., Song, Y., Sun, Y., Xu, H., Liu, W., Jin, Z., Liu, X., Cheng, P., Liu, Y., Ai, L., Li, X., Yan, L., Shi, Z., Wang, X., Wu, F., Qiang, X., Dong, J., Lu, F., and Xu, X.: Interplay between the Westerlies and Asian monsoon recorded in Lake Qinghai sediments since 32 ka, Scientific Reports, 2, 619, doi:10.1038/srep00619, 2012.

Anderson, D. M., Overpeck, J. T., and Gupta, A. K.: Increase in the Asian Southwest monsoon during the past four centuries, Science, 297, 596–599, 2002.

Barnett, T. P., Dumenil, L., Schlese, U., and Roeckner, E.: The effect of Eurasian snow cover on global climate, Science, 239, 504–507, 1989.

Chandrasekar, A. and Kitoh, A.: Impact of localized sea surface temperature anomalies over the equatorial Indian Ocean on the Indian summer monsoon, J. Meteorol. Soc. Jpn., 76, 841–853, 1998.

Dansgaard, W.: Stable isotopes in precipitation, Tellus, 16, 436–468, 1964.

Davis, M. E., Thompson, L. G., Yao, T., and Wang, N.: Forcing of the Asian monsoon on the Tibetan Plateau: evidence from high-resolution ice core and tropical coral records, J. Geophys. Res., 110, D04101, doi:10.1029/2004JD004933, 2005.

Duan, A. M. and Wu, G. X.: Role of the Tibetan Plateau thermal forcing in the summer cliamte patterns over subtropical Asia, Clim. Dynam., 24, 793–807, 2005.

Duan, K., Yao, T., and Thompson, L. G.: Low-frequency of southern Asian monsoon variability using a 295-year record from the Dasuopu ice core in the central Himalayas, Geophys. Res. Lett., 31, L16209, doi:10.1029/2004GL020015, 2004.

Duan, K., Thompson, L. G., Yao, T., Davis, M. E., and Mosley-Thompson, E.: A 1000 year history of atmospheric sulfate concentrations in southern Asia as recorded by a Himalayan ice core, Geophys. Res. Lett., 34, L01810, doi:10.1029/2006GL027456, 2007.

Ferranti, L., Slingo, J. M., Palmer, T. N., and Hoskins, B. J.: Relations between interannual and intraseasonal monsoon variability as diagnosed from AMIP integrations, Q. J. Roy. Meteor. Soc., 123, 1323–1357, 1997.

Fleitmann, D., Burns, S. J., Mudelsee, M., Neff, U., Kramers, J., Mangini, A., and Matter, A.: Holocene forcing of the Indian monsoon recorded in a stalagmite from southern Oman, Science, 300, 1737–1739, 2003.

TCD
7, 1871–1905, 2013
Influence of regional precipitation patterns on stable isotopes
H. Pang et al.

Froehlich, K., Kralik, M., Papesch, W., Pank, D., Scheifinger, H., and Stichler, W.: Deuterium excess in precipitation of Alpine regions: moisture recycling, Isot. Environ. Healt. S., 44, 61–70, 2008.

Gadgil, S.: The Indian monsoon and its variability, Annu. Rev. Earth Pl. Sc., 31, 429–467, 2003.

Gadgil, S. and Asha, G.: Intraseasonal variations of the Indian summer monsoon, Part I: Observational aspects, J. Meteorol. Soc. Jpn., 70, 517–527, 1992.

Goswami, B. N.: South Asian monsoon, in: Intraseasonal Variability of the Atmosphere–Ocean Climate System, edited by: Lau, W. K. M. and Waliser, D. E., Springer, Berlin Heidelberg, 19–61, 2005.

Goswami, B. N., Ajayamohan, R. S., Xavier, P. K., and Sengupta, D.: Clustering of synoptic activity by Indian summer monsoon intraseasonal oscillations, Geophys. Res. Lett., 30, 1431, doi:10.1029/2002GL016734, 2003.

Gupta, A., Rathore, L. S., Singh, S. V., and Mendiratta, N.: Performance of a global circulation model in predicting the winter systems and associated precipitation over North West India during 1994–97, in: The Himalayan Environment, edited by: Dash, S. K. and Bahadur, J., New Age International, 123–138, 1999.

Holdsworth, G., Fogarasi, S., and Krouse, H. R.: Variation of the stable isotopes of water with altitude in the Saint Elias Mountains of Canada, J. Geophys. Res., 96, 7483–7494, 1991.

Hong, S., Lee, K., Hou, S., Hur, S., Ren, J., Burn, L., Rosman, K., Barbante, C., and Boutron, C.: An 800-year record of atmospheric As, Mo, Sn, and Sb deposition in central Asia in high-altitude ice cores from Mt. Qomolangma (Everest), Himalayas, Environ. Sci. Technol., 43, 8060–8065, 2009.

Hou, S., Qin, D., Wake, C. P., Mayewski, P. A., Ren, J., and Yang, Q.: Climatological significance of ice core net-accumulation record at Mt. Qomolangma (Everest), Chinese Sci. Bull., 45, 259–264, 2000.

Hou, S., Qin, D., Zhang, D., Kang, S., Mayewski, P. A., and Wake, C. P.: A 154a high resolution ammonium record from the Rongbuk Glacier, north slope of Mt. Qomolangma (Everest), Tibet-Himal region, Atmos. Environ., 37, 721–729, 2003.

Hou, S., Chappellaz, J., Jouzel, J., Chu, P. C., Masson-Delmotte, V., Qin, D., Raynaud, D., Mayewski, P. A., Lipenkov, V. Y., and Kang, S.: Summer temperature trend over the past two millennia using air content in Himalayan ice, Clim. Past, 3, 89–95, doi:10.5194/cp-3-89-2007, 2007.

Kaplan, A., Cane, M., Kushnir, Y., Clement, A., Blumenthal, M., and Rajagopalan, B.: Analyses of global sea surface temperature 1856–1991, J. Geophy. Res., 103, 18567–18589, 1998.

Kaspari, S., Mayewski, P. A., Kang, S., Sneed, S., Hou, S., Hooke, R., Kreutz, K., Introne, D., Handley, M., Maasch, K., Qin, D., and Ren, J.: Reduction in northward incursions of the South Asian monsoon since 1400 AD inferred from a Mt. Everest ice core, Geophy. Res. Lett., 34, L16701, doi:10.1029/2007GL030440, 2007.

Kaspari, S., Hooke, R., Mayewski, P. A., Kang, S., Hou, S., and Qin, D.: Snow accumulation rate on Mt. Everest: synchroneity with sites across the Tibetan Plateau on 50–100 year timescales, J. Glaciol., 54, 343–352, 2008.

Kaspari, S., Mayewski, P. A., Handley, M., Kang, S., Hou, S., Sneed, S., Maasch, K., and Qin, D.: A high-resolution record of atmospheric dust composition and variability since 1650 AD from a Mt. Everest ice core, J. Climate, 22, 3910–3925, doi:10.1175/2009JCLI2518.1, 2009a.

Kaspari, S., Mayewski, P. A., Handley, M., Kang, S., Sneed, S., Hou, S., and Qin, D.: recent increases in atmospheric concentrations of Bi, U, Cs, S and Ca from a 350-year Mt. Everest ice core record, J. Geophys. Res., 114, D04302, doi:10.1029/2008JD011088, 2009b.

Kaspari, S., Schwikowski, M., Gysel, M., Flanner, M. G., Kang, S., Hou, S., and Mayewski, P. A.: Recent increase in black carbon concentrations from a Mt. Everest ice core spanning 1860–2000 AD, Geophy. Res. Lett., 38, L04703, doi:10.1029/2010GL046096, 2011.

Kistler, R., Kalnay, E., Collins, W., Saha, S., White, G., Woollen, J., Chelliah, M., Ebisuzaki, W., Kanamitsu, M., Kousky, V., van den Dool, H., Jenne, R., and Fiorino, M.: The NCEP-NCAR 50-year reanalysis: monthly means CD-ROM and documentation, B. Am. Meteorol. Soc., 82, 247–268, 2001.

Kodera, K.: Solar influence on the Indian Ocean monsoon through dynamical processes, Geophy. Res. Lett., 31, L24209, doi:10.1029/2004GL020928, 2004.

Krishnamurthy, V. and Shuka, J.: Intraseasonal and interannual variability of rainfall over India, J. Climate, 13, 4366–4377, 2000.

Lang, T. J. and Barros, A. P.: Winter storms in the central Himalayas, J. Meteorol. Soc. Jpn., 82, 829–844, 2004.

Lin, Z. and Wu, X.: A preliminary analysis about the tracks of moisture transport on the Qinghai-Xizang Plateau, Geogr. Res., 9, 33–40, 1990 (in Chinese with English abstract).

Liu, G.: Hydrometeorological characteristics of the Tibet Plateau, in: Proceedings of the Baltimore Symposium, Atmospheric Deposition, IAHS Publ. No. 179, May 1989, 267–280, 1989.

Ming, J., Cachier, H., Xiao, C., Qin, D., Kang, S., Hou, S., and Xu, J.: Black carbon record based on a shallow Himalayan ice core and its climatic implications, Atmos. Chem. Phys., 8, 1343–1352, doi:10.5194/acp-8-1343-2008, 2008.

Moore, G. W. K., Alverson, K., and Holdsworth, G.: The impact that elevation has on the ENSO signal in precipitation records from the Gulf of Alaska region, Climatic Change, 59, 101–121, 2003.

Naidu, C. V., Durgalakshmi, K., Muni Krishna, K., Ramalingeswara Rao, S., Satyanarayana, G. C., Lakshminarayana, P., and Malleswara Rao, L.: Is summer monsoon rainfall decreasing over India in the global warming era?, J. Geophys. Res., 114, D24108, doi:10.1029/2008JD011288, 2009.

Neff, U., Burns, S. J., Mangini, A., Mudelsee, M., Fleitmann, D., and Matter, A.: Strong coherence between solar variability and the monsoon in Oman between 9 and 6 kyr ago, Nature, 411, 290–293, 2001.

Palmer, T. N.: Chaos and predictability in forecasting the monsoons, Proceedings of the Indian National Science Academy A, 60, 57–66, 1994.

Pang, H., Hou, S., Kaspari, S., Mayewski, P. A., Introne, D., Masson-Delmotte, V., Jouzel, J., Li, Z., He, Y., and Qin, D.: Atmospheric circulation change in the central Himalayas indicated by a high-resolution ice core deuterium excess record, Clim. Res., 53, 1–12, 2012.

Prasad, K. D. and Bansod, S. D.: Interannual variations of outgoing longwave radiation and Indian summer monsoon rainfall, Int. J. Climatol., 20, 1955–1964, 2000.

Raju, P. V. S., Mohanty, U. C., Rao, P. L. S., and Bhatla, R.: The contrasting features of Asian summer monsoon during surplus and deficient rainfall over India, Int. J. Climatol., 22, 1897–1914, 2002.

Rao, P. L. S.: Circulation characteristics over the Himalayas during winter season, Meteorol. Atmos. Phys., 83, 19–33, 2003.

Saji, N. H., Goswami, B. N., Vinayachandran, P. N., and Yamagata, T.: A dipole mode in the tropical Indian Ocean, Nature, 401, 360–363, 1999.

Shrestha, M. L.: Interannual variation of summer monsoon rainfall over Nepal and its relation to Southern Oscillation index, Meteorol. Atmos. Phys., 75, 21–28, 2000.

Sikka, D. R. and Gadgil, S.: On the maximum cloud zone and the ITCZ over Indian longitudes during the southwest monsoon, Mon. Weather Rev., 108, 1840–1853, 1980.

Singh, N., Pant, G. B., and Mulye, S. S.: Spatial variability of aridity over northern India, P. Indian AS-Earth, 101, 201–213, 1992.

TCD
7, 1871–1905, 2013

Influence of regional precipitation patterns on stable isotopes

H. Pang et al.

Sontakke, N. A. and Singh, N.: Longest instrumental regional and all-India summer monsoon rainfall series using optimum observations: reconstruction and update, The Holocene, 6, 315–331, 1996.

Sontakke, N. A., Singh, N., and Singh, H. N.: Instrumental period rainfall series of the Indian region (1813–2005): revised reconstruction, update and analysis, The Holocene, 18, 1055–1066, 2008.

Subbaramayya, I. and Naidu, C. V.: Spatial variations and trends in the Indian monsoon rainfall, Int. J. Climatol., 12, 597–609, doi:10.1002/joc.3370120606, 1992.

Thompson, L. G., Yao, T., Mosley-Thompson, E., Davis, M. E., Henderson, K. A., and Lin, P. N.: A high-resolution millennial record of the south Asian monsoon from Himalayan ice cores, Science, 289, 1916–1919, 2000.

Tian, L., Yao, T., Sun, W., Stievenard, M., and Jouzel, J.: Relationship between δD and δ^{18}O in precipitation from north to south of the Tibetan Plateau and moisture cycling, Sci. China Ser. D, 44, 789–796, 2001.

Tian, L., Yao, T., Schuster, P. F., White, J. W. C., Ichiyanagi, K., Pendall, E., Pu, J., and Yu, W.: Oxygen-18 concentrations in recent precipitation and ice cores on the Tibetan Plateau, J. Geophys. Res., 108, 4293, doi:10.1029/2002JD002173, 2003.

Tian, L., Yao, T., White, J. W. C., Yu, W., and Wang, N.: Westerly moisture transport to the middle of Himalayas revealed from the high deuterium excess, Chinese Sci. Bull., 50, 1026–1030, 2005.

Tian, L., Yao, T., MacClune, K., White, J., Schilla, A., Vaughn, B., Vachon, R., and Ichiyanagi, K.: Stable isotopic variations in West China: a consideration of moisture sources, J. Geophys. Res., 112, D10112, doi:10.1029/2006JD007718, 2007.

Vernekar, A. D., Zhou, J., and Shukla, J. S.: The effect of Eurasian snow cover on the Indian monsoon, J. Climate, 8, 248–266, 1995.

Von Rod, U., Schaaf, M., Michels, K. H., Schulz, H., Berger, W. H., and Sirocko, F.: A 5000-yr record of climate change in varved sediments from the oxygen minimum zone off Pakistan, Northeastern Arabian Sea, Quat. Res, 51, 39–53, 1999.

Waliser, D. E. and Gautier, C.: A satellite-derived climatology of the ITCZ, J. Climate, 6, 2162–2174, 1993.

Wang, P., Yao, T., Tian, L., Wu, G., Li, Z., and Yang, W.: Recent high-resolution glaciochemical record from a Dasuopu firn core of middle Himalayas, Chinese Sci. Bull., 53, 418–425, 2008.

TCD
7, 1871–1905, 2013

Influence of regional precipitation patterns on stable isotopes

H. Pang et al.

Webster, P. J., Magaña, V. O., Palmer, T. N., Shukla, J., Tomas, R. A., Yanai, M., and Yasunari, T.: Monsoons: processes, predictability, and the prospects for prediction, J. Geophys. Res., 103, 14451–14510, 1998.

Wei, K. and Gasse, F.: Oxygen isotopes in lacustrine carbonates of West China revisited: implications for post glacial changes in summer monsoon circulation, Quaternary Sci. Rev., 18, 1315–1334, 1999.

Wu, G., Liu, Y., He, B., Bao, Q., Duan, A., and Jin, F.:, Thermal controls on the Asian summer monsoon, Scientific Reports, 2, 1–7, 2012.

Xu, J., Hou, S., Qin, D., Kaspari, S., Mayewski, P. A., Petit, J. R., Delmonte, B., Kang, S., Ren, J., Chappellaz, J., and Hong, S.: A 108.83-m ice-core record of atmospheric dust deposition at Mt. Qomolangma (Everest), Central Himalaya, Quaternary Res., 73, 33–38, 2010.

Yao, T., Guo, X., Thompson, L. G., Duan, K., Wang, N., Pu, J., Xu, B., Yang, X., and Sun, W.: δ^{18}O record and temperature change over the past 100 years in ice cores on the Tibetan Plateau, Sci. China Ser. D, 49, 1–9, doi:10.1007/s11430-004-5096-2, 2006.

Yao, T., Thompson, L., Yang, W., Yu, W., Gao, Y., Guo, X., Yang, X., Duan, K., Zhao, H., Xu, B., Pu, J., Lu, A., Xiang, Y., Kattel, D. B., and Joswiak, D.: Different glacier status with atmospheric circulations in Tibetan Plateau and surroundings, Nature Clim. Change, 2, 663–667, doi:10.1038/nclimate1580, 2012.

Yasunari, T.: Structure of an Indian Summer Monsoon system with around 40-day period, J. Meteorol. Soc. Jpn., 59, 336–354, 1981.

Ye, T. Z.: Some aspects of the thermal influences of the Qinghai-Tibetan Plateau on the atmospheric circulation, Arch. Meteor. Geophy. A, 31, 205–220, 1982.

Zhang, D., Qin, D., Hou, S., Kang, S., Ren, J., and Mayewski, P. A.: Climatic significance of δ^{18}O records from an 80.36 m ice core in the East Rongbuk Glacier, Mount Qomolangma (Everest), Sci. China Ser. D, 48, 266–272, 2005.

Zhang, S., Hou, S., Ma, X., Qin, D., and Chen, T.: Culturable bacteria in Himalayan glacial ice in response to atmospheric circulation, Biogeosciences, 4, 1–9, doi:10.5194/bg-4-1-2007, 2007.

Zhang, S., Hou, S., Wu, Y., and Qin, D.: Bacteria in Himalayan glacial ice and its relationship to dust, Biogeosciences, 5, 1741–1750, doi:10.5194/bg-5-1741-2008, 2008.

Zhang, Q., Wu, G., and Qian, Y.: The bimodality of the 100 hPa south Asia high and its relationship to the climate anomaly over east Asia in summer, J. Meteorol. Soc. Jpn., 80, 733–744, 2002.

TCD
7, 1871–1905, 2013

Zhao, P. and Chen, L. X.: Interannual variability of atmospheric heat source/sink over the Qinghai-Xizang (Tibetan) Plateau and its relation to circulation, Adv. Atmos. Sci., 18, 106–116, 2001.

Table 1. EOF analysis of the instrumental area-averaged summer monsoon (June to September) rainfall series of Indian zones and the ER and Dasuopu $\delta^{18}O$ and accumulation rate records over the period 1848–1996.

	EOF1	EOF2	EOF3	EOF4	EOF5	EOF6	EOF7	EOF8
AISMR	**0.83**	−0.44	−0.03	−0.28	−0.09	0.04	−0.08	−0.03
NEI	0.02	0.03	−0.02	0.05	**−0.99**	−0.01	0.06	0.07
NCI	**0.78**	0.13	−0.42	0.02	−0.21	0.10	−0.14	−0.10
NWI	**0.81**	−0.41	0.17	−0.08	0.17	−0.04	−0.06	0.03
NMI	**0.88**	−0.04	0.02	0.02	0.04	−0.06	0.12	0.05
WPI	0.24	**−0.84**	0.09	−0.30	0.02	0.01	−0.02	0.00
EPI	0.28	**−0.77**	−0.24	0.09	0.02	0.12	−0.13	−0.07
SPI	0.18	−0.19	0.04	**−0.94**	0.06	0.04	−0.05	−0.08
DSP-$\delta^{18}O$	−0.10	0.12	**0.85**	−0.04	0.01	0.26	−0.23	−0.14
DSP-accumulation	0.00	0.12	−0.20	0.04	−0.01	**−0.95**	0.14	0.04
ER-$\delta^{18}O$	0.01	−0.05	0.10	−0.08	0.07	0.04	0.07	**−0.98**
ER-accumulation	0.06	−0.14	0.18	−0.05	0.07	0.14	**−0.94**	0.08
Total variance (%)	24.4	14.7	9.0	9.0	8.9	8.5	8.5	8.4
EOFs interpretations	the core Indian monsoon region rainfall	the middle Indian peninsula rainfall	DSP-$\delta^{18}O$	the southern India peninsula rainfall	the northeastern India peninsula rainfall	DSP-accumulation	ER-accumulation	ER-$\delta^{18}O$

Note: The rotation method, maximum variance of variable, is used when performing EOF analysis. The loaded variables are in bold.

TCD
7, 1871–1905, 2013

Discussion Paper | Discussion Paper | Discussion Paper | Discussion Paper |

TCD

7, 1871–1905, 2013

Influence of regional precipitation patterns on stable isotopes

H. Pang et al.

Table 2. Pearson correlation coefficients between the summer monsoon rainfall over the Indian zones and the ER and Dasuopu δ^{18}O and accumulation rate records since 1813 AD.

	AISMR	NEI	NCI	NWI	NMI	WPI	EPI	SPI	ER-accum	DSP-accum	ER-δ^{18}O	DSP-δ^{18}O
AISMR	1											
NEI	0.09	1										
NCI	0.65[a]	0.19[b]	1									
NWI	0.89[a]	−0.17[b]	0.46[a]	1								
NMI	0.67[a]	0.01	0.54[a]	0.62[a]	1							
WPI	0.634[a]	−0.06	0.05	0.57[a]	0.22[a]	1						
EPI	0.57[a]	−0.08	0.27[a]	0.46[a]	0.30[a]	0.52[a]	1					
SPI	0.53[a]	−0.09	0.10	0.31[a]	0.20[b]	0.42[a]	0.24[a]	1				
ER-accum	0.18[b]	−0.01	0.02	0.20[b]	0.00	0.20[a]	0.17[b]	0.14[c]	1			
DSP-accum	−0.14[c]	0.01	0.01	−0.09	0.02	−0.14[c]	−0.12	−0.14[c]	−0.31[a]	1		
ER-δ^{18}O	0.06	−0.12	0.03	0.02	0.01	0.06	0.03	0.16[b]	0.01	0.10	1	
DSP-δ^{18}O	−0.05	−0.06	−0.25[a]	−0.02	−0.15[c]	−0.07	−0.15	0.11	0.28[a]	−0.39[a]	0.16[b]	1

Note: 2-tailed test of significance is used.
[a] 99 % confidence level.
[b] 95 % confidence level.
[c] 90 % confidence level.
DSP: Dasuopu.

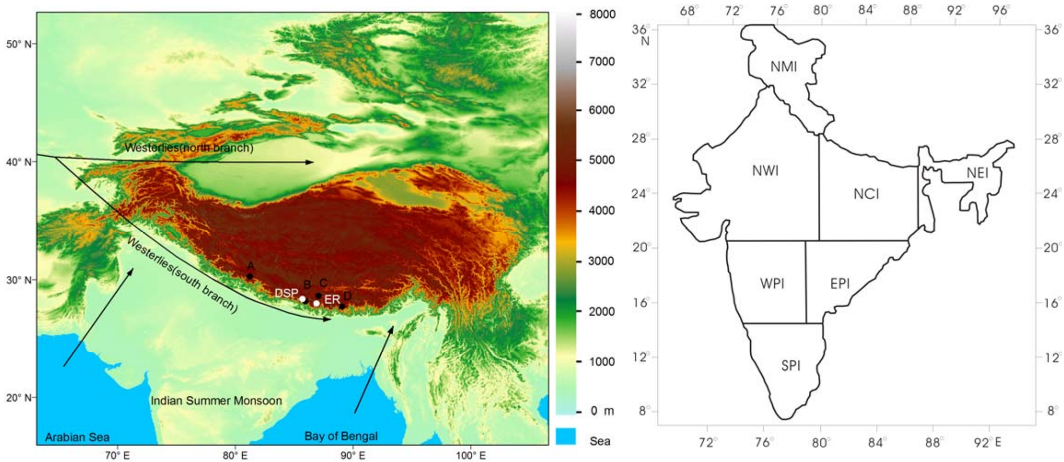

Fig. 1. Atmospheric circulation patterns over the study area (left) and boundary of seven homogeneous rainfall zones of India (right) (redrawn from the reference Sontakke et al., 2008). The black solid circles indicate weather station (A: Pulan; B: Nyalam; C: Dingri; D: Pali), and the white solid circles are ice core sites (DSP: Dasuopu core; ER: East Rongbuk core).

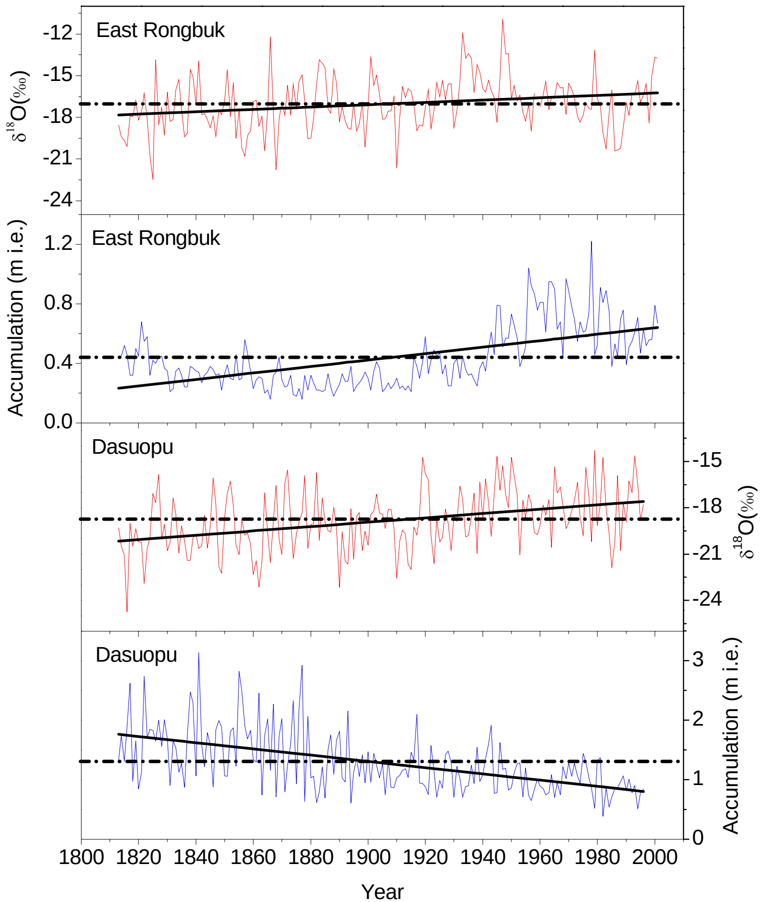

Fig. 2. Ice-core δ^{18}O and accumulation rate time series since 1813 AD from the East Rongbuk and Dasuopu cores. The short dash dot lines are the averages of each series, and the bold lines are linear trends.

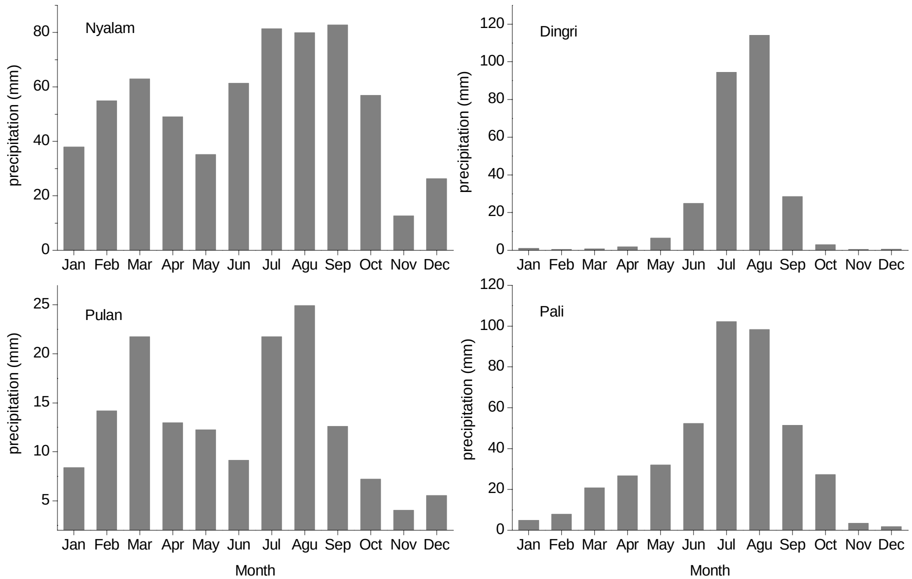

Fig. 3. Monthly longterm mean of precipitation at four weather stations along the Himalayas (Nyalam, Pulan, Dingri and Pali). Seasonal distribution of precipitation is calculated based on the meteorological data observed from July 1966 to November 2011 at Nyalam, January 1973 to November 2011 at Pulan, January 1959 to November 2011 at Dingri and February 1956 to November 2011 at Pali.

TCD
7, 1871–1905, 2013

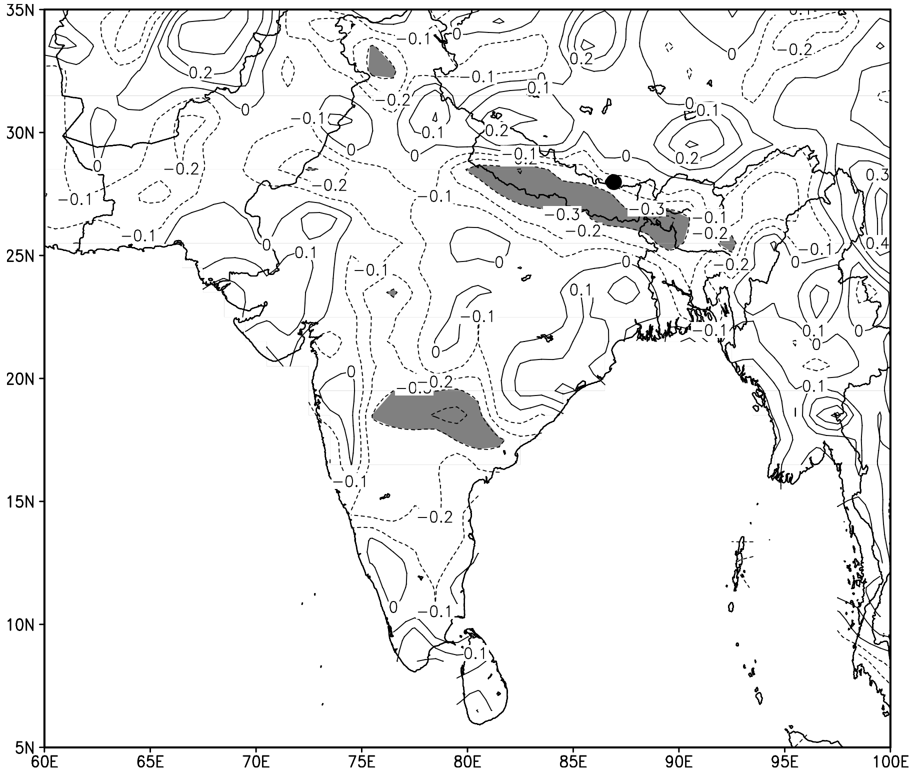

Fig. 4. Correlation coefficients between the ER δ^{18}O record and summer (June–September) precipitation over the period 1951–2001. Grey shadow indicates correlation significance at 95 % confidence level. The solid circle indicates the ER core drilling site. Summer precipitation data is derived from Global Precipitation Climatology Centre (GPCC) monthly precipitation dataset from 1951–present (available at http://gpcc.dwd.de).

TCD
7, 1871–1905, 2013

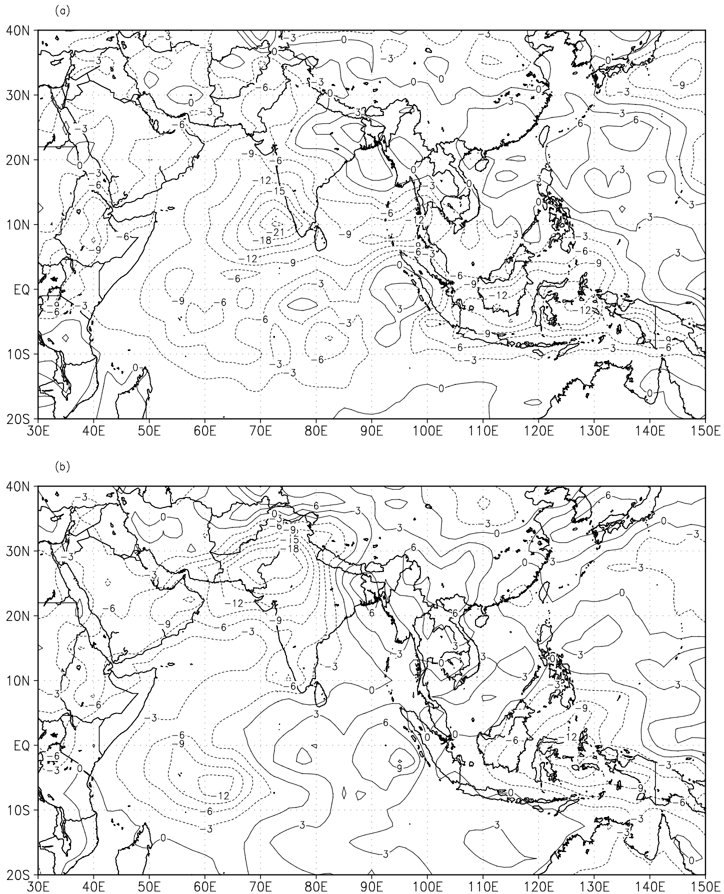

Fig. 5. Difference of summer mean outgoing longwave radiation (OLR) between years with higher and lower SPI precipitation **(a)** and NWI precipitation **(b)** (higher – lower).

TCD
7, 1871–1905, 2013

Influence of regional precipitation patterns on stable isotopes

H. Pang et al.

Title Page
Abstract | Introduction
Conclusions | References
Tables | Figures
◀ | ▶
Back | Close
Full Screen / Esc
Printer-friendly Version
Interactive Discussion

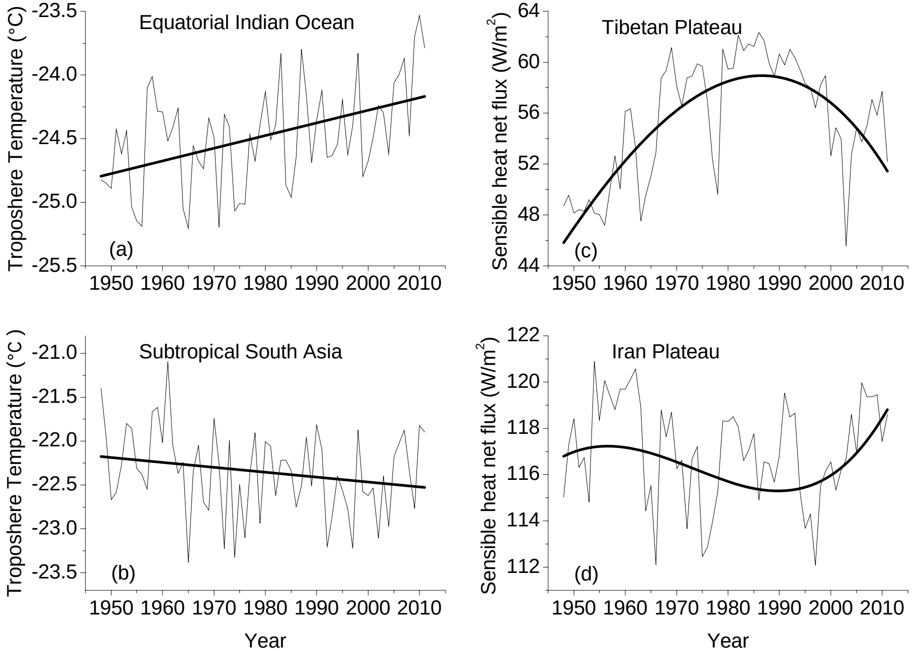

Fig. 6. Variations of mid-upper troposphere summer mean (June–September) temperature **(a)** over the equatorial Indian Ocean (50–100° E; 10° S–10° N) and **(b)** over the subtropical south Asia (50–100° E; 25–40° N), and sensible heat net flux **(c)** on the Tibetan Plateau (80–102.5° E; 27.5–40° N) and **(d)** on the Iran Plateau (50–70° E; 27.5–37.5° N) during 1948–2011. The solid lines indicate the linear trends and the curves are the five polynomial fits.

TCD
7, 1871–1905, 2013